SUPPLEMENTARY DATA

Supplementary Figure 1. Structure of 5-PAHSA. Number 5 marks the branching point. The experiments were performed with a racemic mixture.

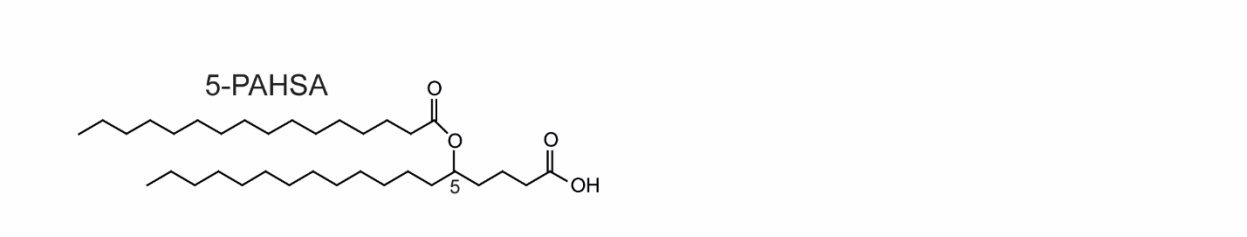

SUPPLEMENTARY DATA

Supplementary Figure 2. (A) Metabolism of TAG 48:1 in eWAT. Fractional synthesis and total levels of metabolites related to TAG 48:1 metabolism. DAG 32:1, diacylglycerol 16:0-16:1. T, significant effect of temperature factor. Two way ANOVA, multiple comparison tests (Sidak), planned multiple comparison of the effect of 5-PAHSA at the given temperature statistically different at $p < 0.05$. (B) Levels of DAGs related to Figure 2G. Two way ANOVA, multiple comparison tests (Tukey), all pairwise, *, $p < 0.05$. $n = 8–9$, mean ± SEM.

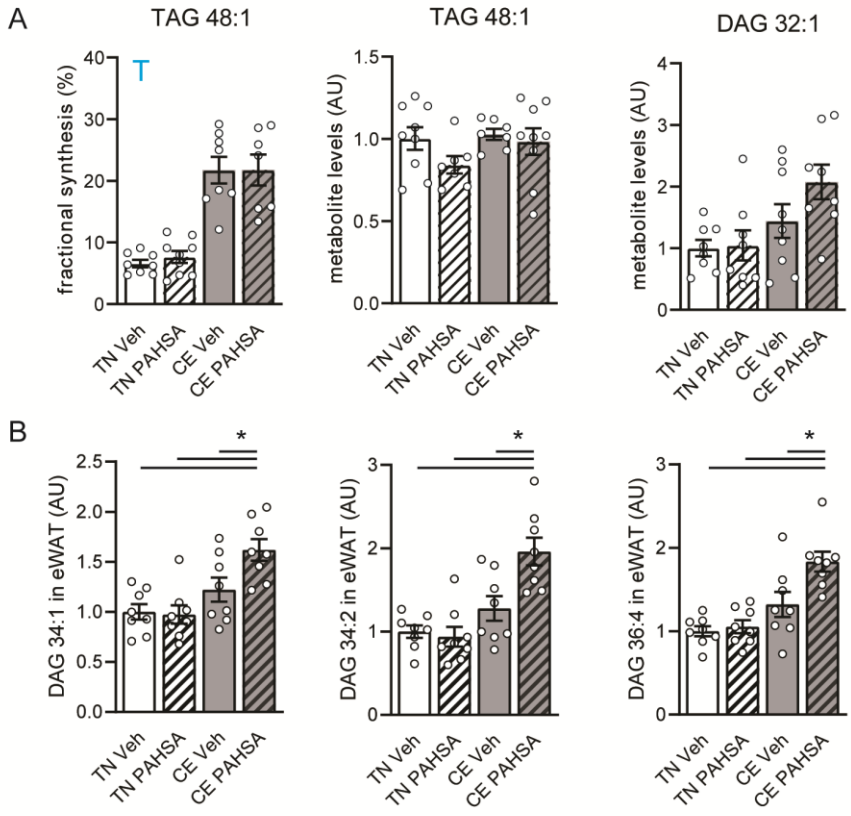

SUPPLEMENTARY DATA

Supplementary Figure 3. (A) MS/MS spectra of TAG-estolide synthetic standard (left) and MS/MS spectra of a mixture of TAG-estolides extracted from mouse WAT (right) acquired at different normalized collision energies (NCE). The TAG-estolides [$R_1/R_2/R_3$-(O-R_4)] were detected as ammonium adducts $[M+NH_4]^+$. At low NCE, a fatty acid esterified to a hydroxy fatty acid is lost as neutral ammonium adduct [R_4+NH_3]. Fragmentation of remaining TAG-like $[M+H]^+$ ion generates also a fragment corresponding to a loss of dehydrated hydroxy fatty acid $[M -R_4{\cdot}NH_3 -R_3\text{-}H_2O]^+$. This fragmentation was considered as a signature pattern for TAG-estolides containing FAHFAs.

The peak *m/z* 1131.0243 represents a mixture of several TAG-estolides in which the major component is TAG EST 16:0_18:2_18:0;1-(O-16:0) and the minor components contain 16:0 / 18:0 / 18:1 / 18:2 and (-O-18:1) acyls.

Figure S3
A:Mass spectra of TAG-estolides

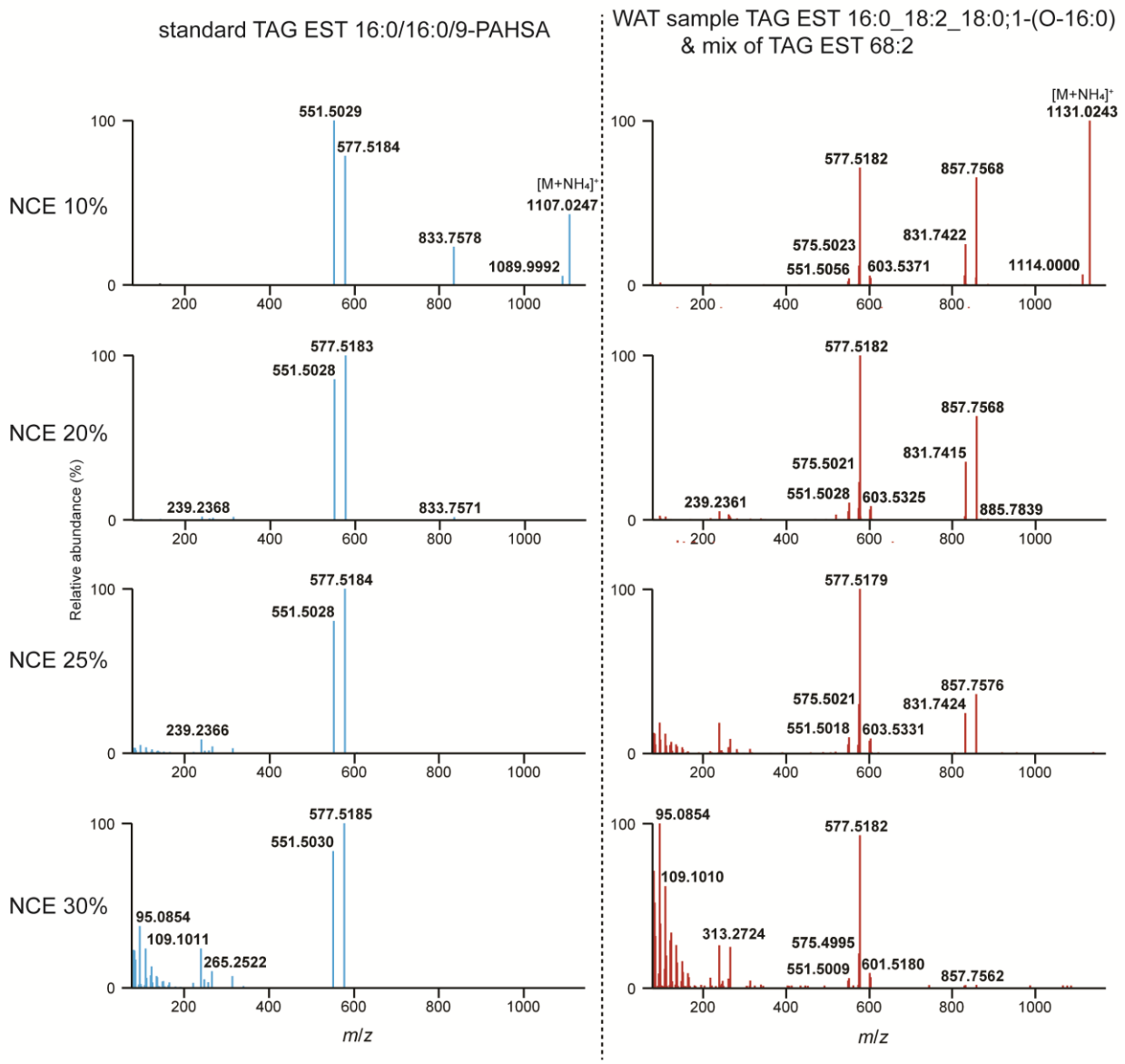

SUPPLEMENTARY DATA

Supplementary Figure 4. Annotation of M+3 isotopologue of TAGs. (A) Mature adipocytes 3T3L-1 were grown in standard media, media with 5.5 mM $^{13}C_6$ glucose, or 5.5 mM $^{13}C_6$ glucose and 1 µM forskolin for 12 hours. Cells were extracted for lipidomics, an aliquot hydrolyzed in KOH and an aliquot measured for intact lipids. (B) Mass distribution per isotopologues of TAG-hydrolyzed palmitic acid in the absence and presence of forskolin. Acetyl-CoA (two carbon) building blocks are visible mainly in the group without forskolin. (C) Schematic fragmentation of TAG 48:0 highlighting M+3 isotopologue, the 3 carbon unit forming glycerol backbone. (D) MS/MS spectra explaining that M+3 ion of TAG 48:0 contains $^{13}C_3$-labeled DAG with the glycerol backbone coming from $^{13}C_6$ glucose.
(E) Glycerol and NEFA levels in media from 3T3-L1 adipocytes similar to the experiment in Figure 4C. Cell were either kept in incubation media (Control and ISO) or pre-incubated with 40 µM 5-PAHSA for 15 min, all cells but control cells stimulated with 10 µM isoproterenol for 2 hours and media collected. (F) Freshly isolated adipocytes from eWAT (C57BL6/J, males, 8 weeks old) were processed as 3T3-L1 adipocytes above. Iso, isoproterenol. Data are means ± SEM; $n = 4$; *, statistically different at $p < 0.05$ by ANOVA, Dunnett multiple comparisons with Iso group set as control. (G) Fatty acid profile of media from the panel F. Numbers in the cells represent fold change over the control group for individual fatty acids, highlighted also as a heatmap.

SUPPLEMENTARY DATA

Figure S4. Identification of M+3 isotopologue as glycerol backbone-containing fragment

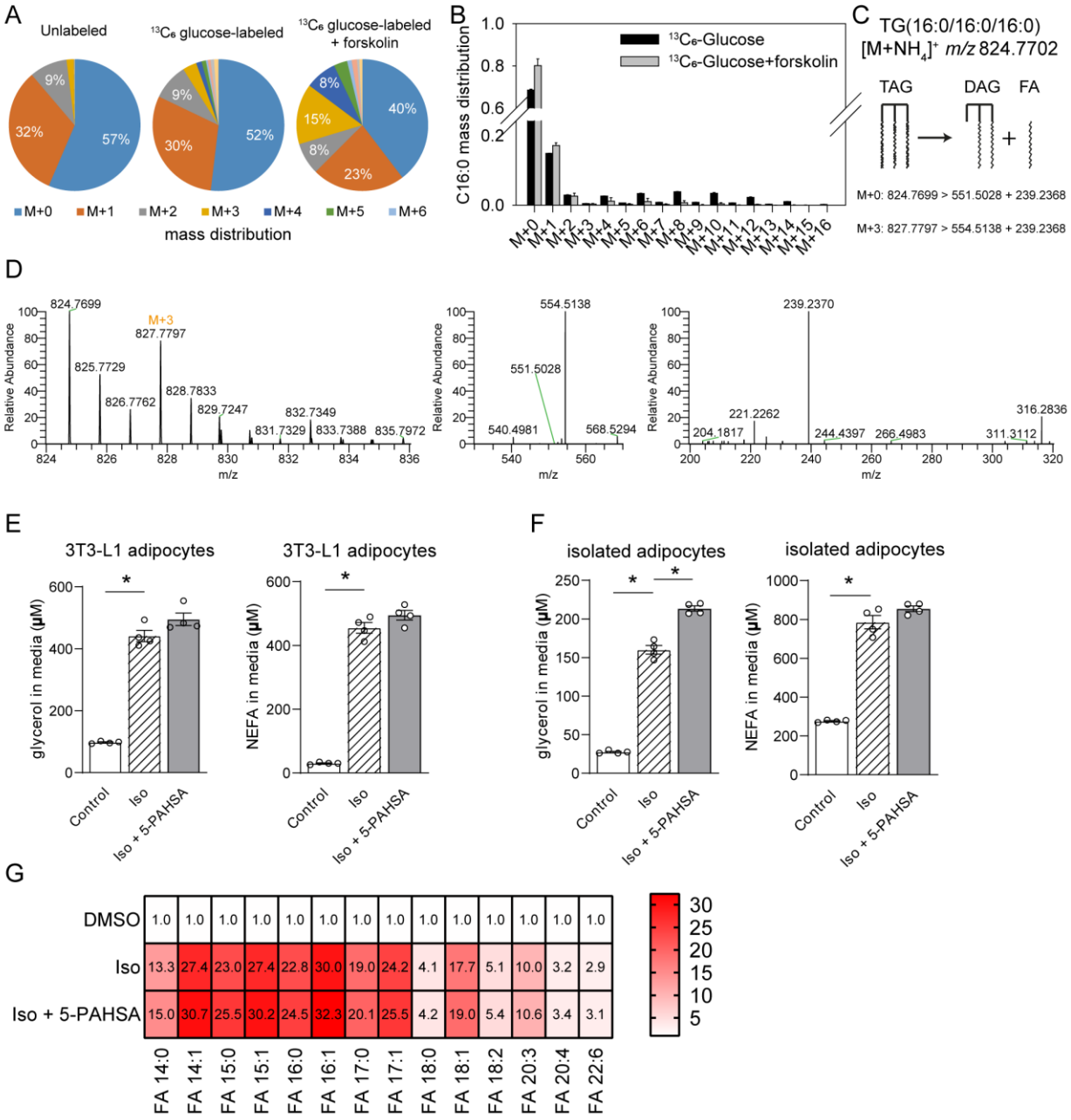

SUPPLEMENTARY DATA

Supplementary Figure 5. Use of [4-^{2}H]-glucose to label NADPH. [4-^{2}H]-glucose can be used as a malic enzyme tracer, which specifically labels NADPH's redox active hydrogen. The deuteron from [4-^{2}H]-glucose is passed to NAD^{2}H by glyceraldehyde 3-phosphate dehydrogenase (*GAPDH*) during glycolysis. This cytosolic NAD^{2}H can be used by cytosolic malate dehydrogenase 1 (*MDH*) to convert cytosolic oxaloacetate (coming from citrate cleavage by ATP citrate lyase) to cytosolic [2-^{2}H]-malate. This deuterated malate can be either transported to mitochondria or converted by malic enzyme 1 (*ME1*) to cytosolic pyruvate and cytosolic NADP^{2}H. This NADP^{2}H represents the energy for DNL. During the synthesis of a fatty acid from acetyl-CoA units (via malonyl-CoA), two NADPH molecules are used per one C_2 unit. The fatty acid labeling is the result of two stochastic hydrogen selection processes, with 1/3 of hydrogens coming from water and 2/3 coming from NADPH. If cytosolic NADP^{2}H is present, contribution of malic enzyme 1 NADPH to fatty acid synthesis can be measured (1-4).

3T3-L1 differentiated adipocytes were incubated with or without 40 µM 5-PAHSA in medium with [4-^{2}H]-glucose for 24 hours without insulin, metabolism quenched on liquid nitrogen, cells extracted to preserve NADPH and NADP+ ratio, and raw extracts immediately measured by LC-MS/MS according to a published protocol (2).

Malate labeling M+1 documents that the deuteron was introduced by labeled NADH. For further details regarding malate labeling and its alternative fate see ref. Lewis et al. (4). NADPH M+1 over NAPD+ M+1 labeling represent the redox-active deuteron on NADP^{2}H. 5-PAHSA treatment resulted in significantly higher labeling of cytosolic NADPH. For more details see ref. Lie et al. (2).

Data are means ± SEM; n = 6; *, statistically different at $p < 0.05$ by Students t-test. Scheme adapted from Lewis et al. (4). Data from this labeling experiments were adjusted for C, H, O, N, P natural abundance and tracer purity using IsoCor-2.0.5 (5).

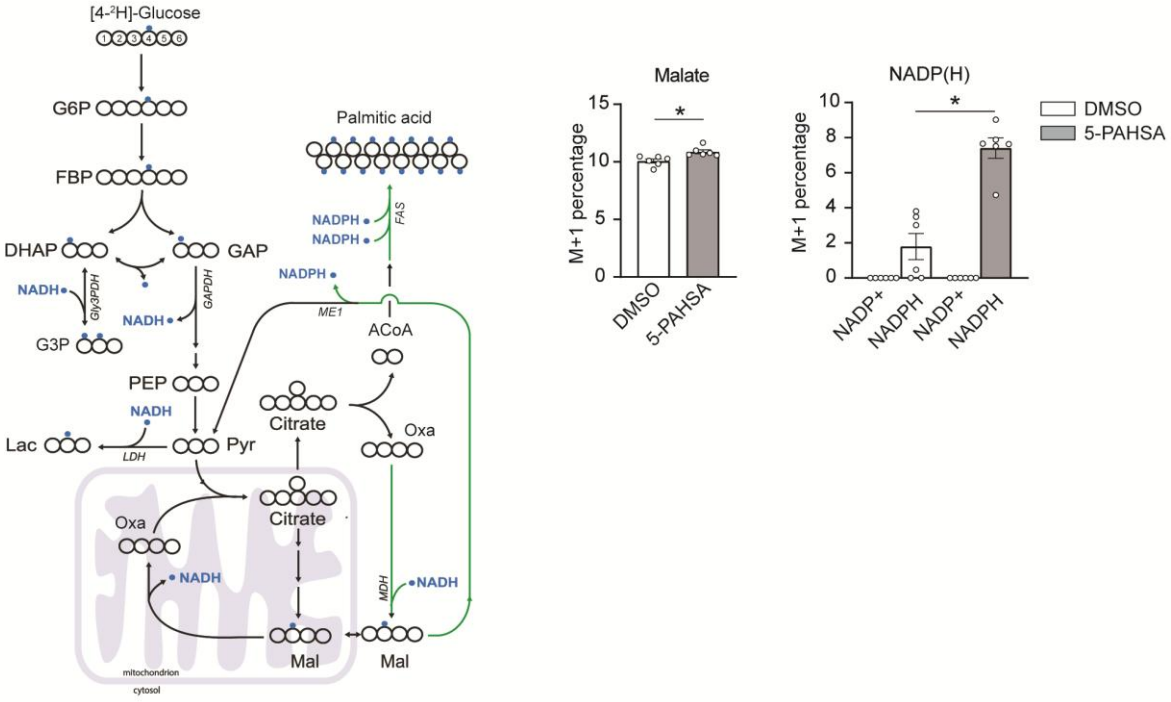

SUPPLEMENTARY DATA

Supplementary Table 1. Figure 3D&E statistics – Two way ANOVA

Metabolite abbreviation	Metabolite annotation	**2way ANOVA**	Interaction	Factor1: FED / FASTED	Factor2: WT / AKO	**Tukey's multiple comparisons test**	fed:WT vs. fed:AKO	fed:WT vs. fasted: WT	fed:WT vs. fasted: AKO	fed:AKO vs. fasted: WT	fed:AKO vs. fasted:AKO	fasted: WT vs. fasted: AKO
Total TAG EST	Total TAG EST in eWAT	Significant?	Yes	Yes	Yes		Yes	Yes	Yes	Yes	No	Yes
TAG EST 68:2	TAG EST 68:2 in eWAT	Significant?	Yes	Yes	Yes		Yes	Yes	Yes	Yes	No	Yes
9-PAHSA	9-PAHSA in eWAT	Significant?	Yes	Yes	Yes		No	Yes	No	Yes	No	Yes
5-PAHSA	5-PAHSA in eWAT	Significant?	Yes	Yes	Yes		No	Yes	No	Yes	No	Yes

SUPPLEMENTARY DATA

Supplementary Table 2. Figure 5B statistics – Two way RM ANOVA

Metabolite abbreviation	Metabolite annotation	**2way RM ANOVA**	Interaction	Factor 1: TIME	Factor 2: DMSO / 5-PAHSA			0 min	5 min	10 min	15 min
Glc	Glucose	Significant?	Yes	Yes	No	**Sidak's multiple comparisons test (DMSO - PAHSA)**	*Is there a difference between DMSO and 5-PAHSA at specific time points?*	No	No	No	No
G6P+F6P	Glucose-6-Phosphate and Fructose-6-Phosphate	Significant?	No	Yes	No			No	No	No	Yes
6PGC	6-Phosphogluconate	Significant?	Yes	Yes	Yes			No	Yes	No	No
5P5	Pentose-5-Phosphates	Significant?	Yes	No	No			No	No	No	No
UGlc	Uridine diphosphate glucose	Significant?	Yes	Yes	No			No	No	No	No
FBP	Fructose-1,6-bisphosphate	Significant?	No	Yes	Yes			No	No	No	No
S7P	Sedoheptulose-7-Phosphate	Significant?	No	Yes	Yes			No	No	No	No
E4P	Erythrose-4-Phosphate	Significant?	No	Yes	No			No	No	No	No
DHAP+GAP	Dihydroxyacetone phosphate and Glyceraldehyde-3-Phosphate	Significant?	No	Yes	No			No	No	No	No
G3P	Glycerol-3-Phosphate	Significant?	No	Yes	Yes			No	No	No	No
2PG+3PG	2-Phosphoglycerate and 3-Phosphoglycerate	Significant?	Yes	Yes	Yes			No	No	Yes	No
PEP	Phosphoenopyruvate	Significant?	Yes	Yes	Yes			No	No	Yes	No
Pyr	Pyruvate	Significant?	Yes	Yes	Yes			No	No	No	No
Lac	Lactate	Significant?	No	No	Yes			No	No	No	No
Asp	Aspratate	Significant?	Yes	No	Yes			No	No	No	No
Cit	Citrate	Significant?	No	Yes	Yes			No	No	No	No
Glu	Glutamate	Significant?	No	Yes	Yes			No	No	No	No
Suc	Succinate	Significant?	No	Yes	No			No	No	No	No
Fum	Fumarate	Significant?	No	Yes	No			No	No	No	No
Mal	Malate	Significant?	No	Yes	No			No	No	No	No

SUPPLEMENTARY DATA

Supplementary Table 3. Figure 5C statistics – Two way RM ANOVA

Metabolite abbreviation	Metabolite annotation	**2way ANOVA**	Interaction	Factor1: A / B	Factor2: C / D		A:D vs. A:C	A:D vs. B:D	A:D vs. B:C	A:C vs. B:D	A:C vs. B:C	B:D vs. B:C
6GP	6-Phosphogluconate	Significant?	No	No	Yes	**Tukey's multiple comparisons test**	Yes	No	No	Yes	No	No
E4P	Erythrose-4-Phosphate	Significant?	No	No	Yes		Yes	No	Yes	Yes	No	Yes
DHAP+GAP	Dihydroxyacetone phosphate and Glyceraldehyde-3-Phosphate	Significant?	Yes	Yes	Yes		No	Yes	Yes	Yes	Yes	Yes
G3P	Glycerol-3-Phosphate	Significant?	Yes	Yes	Yes		No	Yes	Yes	Yes	Yes	Yes
2PG+3PG	2-Phosphoglycerate and 3-Phosphoglycerate	Significant?	No	Yes	Yes		No	Yes	Yes	Yes	Yes	Yes
PEP	Phosphoenopyruvate	Significant?	No	Yes	Yes		Yes	No	Yes	Yes	Yes	Yes
Pyr	Pyruvate	Significant?	No	Yes	Yes		No	Yes	Yes	Yes	Yes	No
Mal	Malate	Significant?	Yes	Yes	No		No	Yes	Yes	Yes	Yes	No
Cit	Citrate	Significant?	No	Yes	No		No	Yes	Yes	Yes	Yes	No

Factors: A: NONE, B: INSULIN, C: DMSO, D: 5-PAHSA

SUPPLEMENTARY DATA

Methods

REAGENT or RESOURCE	SOURCE	IDENTIFIER
Chemicals, Peptides, and Recombinant Proteins		
[U-^{13}C]-Glucose	Cambridge Isotopes	CLM-1396-1
[U-^{13}C]-Glutamine	Cambridge Isotopes	CLM-1822-H-PK
Deuterium oxide	CortecNET	CD5253P1000
[4-^{2}H]-Glucose	Cambridge Isotopes	DLM-9294-PK
$^{13}C_4$-9-PAHSA	Cayman chemicals	17725
5-PAHSA	(6)	N/A
DMSO, dry	Sigma	41647
PEG-400	Sigma	202398
Tween-80	Sigma	P4780
SPE columns 500 mg / 10 mL	Thermo	60108-793
BTSF	Sigma	15238
DMEM	Sigma	D5796
DMEM	GIBCO	A1443001
DMEM powder	Sigma	D5648
Fetal bovine serum	Sigma	F7524
Bovine serum albumin, for cell culture	Sigma	A8806
Atglistatin	Sigma	SML1075
Forskolin	Sigma	F3917
TRI reagent	Sigma	T9424
Insulin	Sigma	I9278
Critical Commercial Assays		
NEFA-HR kit	FUJI	434-91795
RANDOX glycerol kit	RANDOX	GY 105
Experimental Models: Cell Lines		
3T3-L1	ATCC	USA
Experimental Models: Organisms/Strains		
C57BL/6JBomTac	Taconic Biosciences	Denmark
C57BL/6J, global ATGL knockout	University of Graz / R. Zechner	Austria
Oligonucleotides		
Primers used for qPCR	(7)	N/A
Software and Algorithms		
GraphPad Prism 8.0	GraphPad Software	https://www.graphpad.com/
MS-DIAL 3.52	(8)	http://prime.psc.riken.jp/Metabolomics Software/MS-DIAL/
IsoCor	(5)	https://pypi.org/project/IsoCor/
EnviPat web & R package	(9)	https://www.envipat.eawag.ch/index.php
Other		
Chow, extruded Ssniff R/M-H	Ssniff Spezialdiaten GmbH	Germany

SUPPLEMENTARY DATA

Animal Studies

Two-month-old-male B6 (C57BL/6JBomTac, Taconic Biosciences, Ejby, Denmark) mice fed standard chow (extruded Ssniff R/M-H from Ssniff Spezialdiaten GmbH, Soest, Germany; metabolizable energy 13 MJ kg^{-1}) were maintained close to thermoneutrality (that is, at 30°C) for 1 week. Thereafter, subgroups of mice were either maintained at 30°C (control animals) or exposed to cold (6°C for 7 days) before killing (10). After 3 days, mice were further divided into subgroups and received an oral gavage of 5-PAHSA or saline (in PEG-400/Tween-80 formulation (11)). The 5-PAHSA dose was 45 mg/kg. Animals were caged in groups of 3–4 and all mice from the same cage were killed at the same time during the experiment, under ether anesthesia in a randomly fed state (between 08:00 and 10:00 hr). EDTA-plasma and various tissues were collected, including liver, eWAT and dorso-lumbar WAT. Samples were flash-frozen and stored in liquid nitrogen.

Data for Figure 1A-D and F-G were acquired from two independent cohorts. Data for Figure 3G (TAG EST 68:2 levels) were acquired from an independent cohort (C57BL/6JBomTac, males, cold exposure/thermoneutrality protocol as above). A separate cohort of mice was used for Figure S4G experiment (C57BL/6JBomTac, males, 8 weeks old on chow diet).

All experiments were approved by the Animal Care and Use Committee of the Institute of Physiology of the Czech Academy of Sciences and followed the guidelines.

Global ATGL knockout (AKO) mice were generated by breeding heterozygous AKO mice (12; 13). AKO mice were backcrossed into C57BL/6J for > 10 generations. All animal protocols were approved by the Austrian Federal Ministry for Science, Research, and Economy (protocol numbers BMWF-66.007/0017/-II/3b/2013 and BMWFW-66.007/0006/-WF/V/3b/2014) and the ethics committee of the University of Graz, and were conducted in compliance with the council of Europe Convention (ETS 123). Mice were bred and maintained under specific pathogen free conditions. Cages and water were autoclaved, and regular chow diet (R/M-H Extrudate, V1126-037, Ssniff Spezialdiaten GmbH, Soest, Germany). Female mice were fasted for 12 hrs, and dissected (14). Cold exposure experiments – 6 hours of acute cold (AC) exposure and 3 weeks of chronic cold adaptation, *ad libitum* fed mice, were performed as before (14).

5-PAHSA Treatment

It proved critical to sonicate the mixture with 5-PAHSA for gavage in a water bath warmed to 40°C for 30 min before the application and to keep the test tube in an aluminum block heated to 37°C in the cold room to prevent PAHSA precipitation during the gavage procedure.

Preparation of media containing 5-PAHSA proved to be critical for the output of the experiment. 5-PAHSA, dissolved in dry DMSO, was heated in a water bath to 37°C and kept in a Styrofoam tube holder to prevent cooling and precipitation. Appropriate amount, corresponding to max. 0.1% volume of the media, was dissolved in the experimental DMEM. It was necessary to sonicate the media in a water bath heated to 40°C for at least 30 min till the media turned clear and to keep the media at 37°C till the plates were stored in the incubator. The concentration of 40 μM 5-PAHSA, yielding consistent effects, was selected based on glucose uptake screening experiments (not shown). Growing cell with 5-PAHSA for 3 days induced mRNA levels of Glut4 (similar to (15), but other lipogenic genes (Acly, Fasn, Pck1) were not significantly affected (not shown).

Sample Extraction

Extraction of metabolites was carried out using a biphasic solvent system of cold methanol, methyl *tert*-butyl ether (MTBE), and water (16) with some modifications.

In more detail, 765 μL of cold methanol/MTBE mixture (165 μL + 600 μL, respectively) containing a mixture of odd chain and deuterated lipid internal standards was added to 25 μL blood serum aliquot and shaken for 30 s. Then, 165 μL of 10% MeOH with deuterated polar metabolite internal standards was added, shaken for 30 s, and centrifuged at 16,000 rpm for 5 min. An aliquot of 100 μL of upper organic phase was collected, evaporated, resuspended in 100 μL of methanol with [12-[(cyclohexylamino) carbonyl]amino]-dodecanoic acid (CUDA) internal standard, shaken for 30 s, centrifuged at 16,000 rpm

for 2 min and analyzed using lipidomics platforms. Also, an aliquot of 70 µL of bottom aqueous phase was collected, evaporated, resuspended in 70 µL of an acetonitrile/water (4:1, *v*/*v*) mixture with CUDA and Val-Tyr-Val internal standards, shaken for 30 s, centrifuged at 16,000 rpm for 5 min and analyzed using HILIC metabolomics platform.

WAT samples (20 mg) were homogenized with 275 µL MeOH and 275 µL 10% MeOH both containing internal standards for 1.5 min using a grinder (MM400, Retsch, Germany). Then, 1 mL of MTBE with internal standard was added, the tubes were shaken for 1 min and centrifuge at 16,000 rpm for 5 min. For profiling of high-abundant TAG and low-abundant TAG EST, 10 µL of upper organic phase was collected, resuspended using a chloroform/MeOH/isopropanol (1:2:4, *v*/*v*/*v*) mixture, shaken for 30 s, centrifuged at 16,000 rpm for 2 min and used for lipidomics ESI(+) platform for TAG EST while for TAG analysis the extract was further 100-times diluted with methanol containing CUDA internal standard. For profiling of minor-lipid species in positive and negative ion mode, 100 µL of upper organic phase was collected, evaporated, and resuspended using 80% MeOH with CUDA internal standard, shaken for 30 s, centrifuged at 16,000 rpm for 2 min and used LC-MS analysis. An aliquot of 70 µL of bottom aqueous phase was collected, evaporated, resuspended in 70 µL of an acetonitrile/water (4:1, *v*/*v*) mixture with CUDA and Val-Tyr-Val internal standards, shaken for 30 s, centrifuged at 16,000 rpm for 5 min and analyzed using HILIC metabolomics platform. Another 70 µL of bottom aqueous phase was mixed with 210 µL of an isopropanol/acetonitrile (1:1, *v*/*v*) mixture, shaken for 30 s, centrifuged at 16,000 rpm for 5 min, and the supernatant was evaporated, resuspended in 5% MeOH/0.2% formic acid with CUDA and Val-Tyr-Val internal standards, shaken for 30 s, centrifuged at 16,000 rpm for 5 min and analyzed using HSS T3 metabolomics platform.

For extraction of polar metabolites ($NADPH/NADP^+$) from cells, a mixture of 40:40:20 acetonitrile:methanol:water (*v*/*v*/*v*), with the 0.1 M formic acid was used as reported before (2; 3). The extracts were immediately analyzed using HILIC and HSS T3 metabolomics platforms.

LC–MS Analysis

The LC-MS system consisted of a Vanquish UHPLC System (Thermo Fisher Scientific, Bremen, Germany) coupled to a Q Exactive Plus mass spectrometer (Thermo Fisher Scientific).

Lipidomics Platforms

Lipids were separated on an Acquity UPLC BEH C18 column (50 × 2.1 mm; 1.7 µm) coupled to an Acquity UPLC BEH C18 VanGuard pre-column (5 × 2.1 mm; 1.7 µm) (Waters, Milford, MA, USA). The column was maintained at 65°C at a flow-rate of 0.6 mL/min. For LC–ESI(+)-MS analysis, the mobile phase consisted of (A) 60:40 (*v*/*v*) acetonitrile:water with ammonium formate (10 mM) and formic acid (0.1%) and (B) 90:10:0.1 (*v*/*v*/*v*) isopropanol:acetonitrile:water with ammonium formate (10 mM) and formic acid (0.1%). For LC–ESI(−)-MS analysis, the composition of the solvent mixtures were the same with the exception of the addition of ammonium acetate (10 mM) and acetic acid (0.1%) as mobile-phase modifier. Separation was conducted under the following gradient for LC–ESI(+)-MS: 0 min 15% (B); 0–1 min 30% (B); 1–1.3 min from 30% to 48% (B); 1.3–5.5 min from 48% to 82% (B); 5.5–5.8 min from 82% to 99% (B); 5.8–6 min 99% (B); 6–6.1 min from 99% to 15% (B); 6.1–7.5 min 15% (B). For LC–ESI(−)-MS, the following gradient was used: 0 min 15% (B); 0–1 min 30% (B); 1–1.3 min from 30% to 48% (B); 1.3–4.8 min from 48% to 76% (B); 4.8–4.9 min from 76% to 99% (B); 4.9–5.3 min 99% (B); 5.3–5.4 min from 99% to 15% (B); 5.4–6.8 min 15% (B). A sample volume of 2 and 3 µL was used for injection for ESI(+) and ESI(–), respectively. Sample temperature was maintained at 4°C.

The source and MS parameters were sheath gas pressure, 60 arbitrary units; aux gas flow, 25 arbitrary units; sweep gas flow, 2 arbitrary units; capillary temperature, 300°C; aux gas heater temperature, 370°C. For general lipidomics profiling the mass spectrometer was operated under following conditions: MS1 mass range, m/z 200–1700; MS1 resolving power, 35,000 FWHM (*m/z* 200); number of data-dependent scans per cycle, 3; MS/MS resolving power, 17,500 FWHM (*m/z* 200). For ESI(+), a spray voltage of 3.6 kV and normalized collision energy of 20% was used while for ESI(−) a spray voltage of

−3.0 kV and normalized collision energy of 10, 20 and 30% were set-up. For fluxomics lipidomics profiling the instrument acquired MS1 data only at a resolving power of 140,000 FWHM (*m/z* 200).

For TAG EST platform the MS1 mass range of *m*/*z* 1000–1600 was used. Data were acquired at positive ESI mode with a spray voltage of 3.6 kV and normalized collision energy of 20%. Using this methodology, TAG EST mixture could be separated according to the number of carbons and double bonds and individual superfamilies (e.g. 70:4) could be quantified. TAG EST quantification was performed using deuterated TAG internal standards (TAG 51:1-d_5, TG 60:1-d_5) and confirmed by the method of standard addition of pure TAG EST 70:4 (18:2/18:2/9-PAHSA synthesized from 1,2-dilinoleoyl glycerol and 9-PAHSA). FA composition of the TAG EST (or the main contributor) within the superfamily can be deduced from the MS/MS spectra, thus allowing the assessment of TAG EST acyl composition. TAG EST acyl position, chirality or estolide bond branching was not explored.

Metabolomics Platforms

Polar metabolites (serum, WAT) were separated on an Acquity UPLC BEH Amide column (50 × 2.1 mm; 1.7 μm) coupled to an Acquity UPLC BEH Amide VanGuard pre-column (5 × 2.1 mm; 1.7 μm) (Waters, Milford, MA, USA). The column was maintained at 45°C at a flow-rate of 0.4 mL/min. The mobile phase consisted of (A) water with ammonium formate (10 mM) and formic acid (0.125%) and (B) acetonitrile:water (95/5) with ammonium formate (10 mM) and formic acid (0.125%). Separation was conducted under the following gradient: 0 min 100% (B); 0–1 min 100% (B); 1–3.9 min from 100% to 70% (B); 3.9–5.1 min from 70% to 30% (B); 5.1–6.4 min from 30% to 100%(B); 6.4–8.0 min 100% (B). A sample volume of 1 μL was used for injection. Sample temperature was maintained at 4°C.

Polar metabolites (WAT) were also separated on an Acquity UPLC HSS T3 column (50 × 2.1 mm; 1.7 μm) coupled to an Acquity UPLC HSS T3 VanGuard pre-column (5 × 2.1 mm; 1.7 μm) (Waters, Milford, MA, USA). The column was maintained at 45°C using a ramped flow-rate. The mobile phase consisted of (A) water with formic acid (0.2%) and (B) methanol with formic acid (0.1%). Separation was conducted under the following gradient: 0 min 1% (B) 0.3 mL/min; 0–0.5 min 1% (B) 0.3 mL/min; 0.5–2 min from 1% to 60% (B) 0.3 mL/min; 2–2.3 min from 60% to 95% (B) from 0.3 mL/min to 0.5 mL/min; 2.3–3.0 min 95% (B) 0.5 mL/min; 3.0–3.1 min from 95% to 1% (B) 0.5 mL/min; 3.1–4.5 min 1% (B) 0.5 mL/min; 4.5–4.6 min 1% (B) from 0.5 mL/min to 0.3 mL/min; 4.6–5.5 min 1% (B) 0.3 mL/min. A sample volume of 5 μL was used for injection. Sample temperature was maintained at 4°C.

The source and MS parameters were ESI ionization, negative; sheath gas pressure, 50 arbitrary units; aux gas flow, 13 arbitrary units; sweep gas flow, 3 arbitrary units; capillary temperature, 260°C; aux gas heater temperature, 425°C. For general metabolomics profiling the mass spectrometer was operated under following conditions: MS1 mass range, *m/z* 60–900; MS1 resolving power, 35,000 FWHM (*m/z* 200); number of data-dependent scans per cycle, 3; MS/MS resolving power, 17,500 FWHM (*m/z* 200). A spray voltage of 3.6 kV and −2.5 kV for ESI(+) and ESI(–), respectively, was used. For both platforms a normalized collision energy of 20, 30 and 40% were used. For fluxomics metabolomics profiling the instrument acquired MS1 data only at a resolving power of 140,000 FWHM (*m/z* 200).

For analysis of cell metabolites (NADPH/$NADP^+$) modified HILIC platform was used with an Acquity UPLC BEH Amide column (50 × 2.1 mm; 1.7 μm) coupled to an Acquity UPLC BEH Amide VanGuard pre-column (5 × 2.1 mm; 1.7 μm) (Waters, Milford, MA, USA). The column was maintained at 25°C at a flow-rate of 0.3 mL/min. The mobile phase consisted of (A) water with ammonium acetate (20 mM) and ammonium hydroxide (pH 9.45) and (B) acetonitrile. Separation was conducted under the following gradient: 0 min 95% (B); 0–1 min 95% (B); 2–9.5 min from 95% to 30% (B); 9.5–10.5 min from 30% to 5% (B); 10.5–12.5 min at 5% (B), 12.5–16 from 5% to 3% (B); 16–16.1 min from 3% to 95% (B), 16.1–20 min at 95% (B). A sample volume of 5 μL was used for injection. Sample temperature was maintained at 4°C. Conditions of HSS T3 metabolomics platform were the same as described above.

SUPPLEMENTARY DATA

Isolation of Adipocytes of WAT and Lipolysis

Adipocytes were isolated from epididymal WAT according to published method (17; 18) using Krebs-Ringer bicarbonate medium with 5 mM glucose and 4% BSA (fraction V, FA free, SigmaeAldrich). Collagenase-digested samples were passed through a sterile 250 mm nylon mesh and the suspension was centrifuged at 4 g for 5 min. The top buoyant layer was washed and collected as floating adipocytes. Isolated adipocytes were kept in incubation media or pre-incubated with 40 µM 5-PAHSA for 15 min, and then 10 µM isoproterenol (final concentration) was added to cells. Media samples were collected after 2 hours and glycerol and NEFA levels measured.

Lipolysis

3T3-L1 mature adipocytes were serum-starved in DMEM complete medium with 0.1% (w/v) bovine serum albumin for 15 hours, washed and pre-incubated with DMSO, 10 nM insulin, or 40 µM 5-PAHSA in glutamine-free media with 5.5 mM $^{13}C_6$-glucose and 1% BSA for 30 min. Then, forskolin was added to a final concentration of 1 µM. The experiment was terminated after 2 hours, media collected, and cells extracted for metabolite profiling. Media free FA and glycerol were measured as before (10). Alternatively, 3T3-L1 adipocytes were pre-incubated with DMSO or 10 µM Atglistatin (Sigma Aldrich) for 2 hours, washed and further incubated with or without 10 µM forskolin for 2 hours (19). Neither adenosine nor adenosine deaminase were used. An aliquot of media was used for free FA and glycerol measurement, and the content of the well was extracted for FAHFA analysis.

Lipolysis experiment presented in Figure 4E was performed according to previously published conditions (20). Briefly, 3T3-L1 adipocytes were serum-starved, pre-incubated with 5-PAHSA (40 µM), insulin (120 pM), and their combination for 30 min, and further stimulated with 10 nM isoproterenol for 120 min. DMEM with 5 mM glucose and 3 % BSA was used.

References

1. Fan J, Ye J, Kamphorst JJ, Shlomi T, Thompson CB, Rabinowitz JD: Quantitative flux analysis reveals folate-dependent NADPH production. Nature 2014;510:298-302

2. Liu L, Shah S, Fan J, Park JO, Wellen KE, Rabinowitz JD: Malic enzyme tracers reveal hypoxia-induced switch in adipocyte NADPH pathway usage. Nat Chem Biol 2016;12:345-352

3. Zhang Z, Chen L, Liu L, Su X, Rabinowitz JD: Chemical Basis for Deuterium Labeling of Fat and NADPH. J Am Chem Soc 2017;139:14368-14371

4. Lewis CA, Parker SJ, Fiske BP, McCloskey D, Gui DY, Green CR, Vokes NI, Feist AM, Vander Heiden MG, Metallo CM: Tracing compartmentalized NADPH metabolism in the cytosol and mitochondria of mammalian cells. Mol Cell 2014;55:253-263

5. Millard P, Letisse F, Sokol S, Portais JC: IsoCor: correcting MS data in isotope labeling experiments. Bioinformatics 2012;28:1294-1296

6. Balas L, Bertrand-Michel J, Viars F, Faugere J, Lefort C, Caspar-Bauguil S, Langin D, Durand T: Regiocontrolled syntheses of FAHFAs and LC-MS/MS differentiation of regioisomers. Org Biomol Chem 2016;14:9012-9020

7. Adamcova K, Horakova O, Bardova K, Janovska P, Brezinova M, Kuda O, Rossmeisl M, Kopecky J: Reduced Number of Adipose Lineage and Endothelial Cells in Epididymal fat in Response to Omega-3 PUFA in Mice Fed High-Fat Diet. Mar Drugs 2018;16

8. Tsugawa H, Cajka T, Kind T, Ma Y, Higgins B, Ikeda K, Kanazawa M, VanderGheynst J, Fiehn O, Arita M: MS-DIAL: data-independent MS/MS deconvolution for comprehensive metabolome analysis. Nat Methods 2015;12:523-526

9. Loos M, Gerber C, Corona F, Hollender J, Singer H: Accelerated isotope fine structure calculation using pruned transition trees. Anal Chem 2015;87:5738-5744

10. Flachs P, Adamcova K, Zouhar P, Marques C, Janovska P, Viegas I, Jones JG, Bardova K, Svobodova M, Hansikova J, Kuda O, Rossmeisl M, Liisberg U, Borkowska AG, Kristiansen K, Madsen L, Kopecky J: Induction of lipogenesis in white fat during cold exposure in mice: link to lean phenotype. Int J Obes (Lond) 2017;41:372-380

11. Yore MM, Syed I, Moraes-Vieira PM, Zhang T, Herman MA, Homan EA, Patel RT, Lee J, Chen S, Peroni OD, Dhaneshwar AS, Hammarstedt A, Smith U, McGraw TE, Saghatelian A, Kahn BB: Discovery of a class of endogenous mammalian lipids with anti-diabetic and anti-inflammatory effects. Cell 2014;159:318-332
12. Haemmerle G, Lass A, Zimmermann R, Gorkiewicz G, Meyer C, Rozman J, Heldmaier G, Maier R, Theussl C, Eder S, Kratky D, Wagner EF, Klingenspor M, Hoefler G, Zechner R: Defective lipolysis and altered energy metabolism in mice lacking adipose triglyceride lipase. Science 2006;312:734-737
13. Haemmerle G, Moustafa T, Woelkart G, Buttner S, Schmidt A, van de Weijer T, Hesselink M, Jaeger D, Kienesberger PC, Zierler K, Schreiber R, Eichmann T, Kolb D, Kotzbeck P, Schweiger M, Kumari M, Eder S, Schoiswohl G, Wongsiriroj N, Pollak NM, Radner FP, Preiss-Landl K, Kolbe T, Rulicke T, Pieske B, Trauner M, Lass A, Zimmermann R, Hoefler G, Cinti S, Kershaw EE, Schrauwen P, Madeo F, Mayer B, Zechner R: ATGL-mediated fat catabolism regulates cardiac mitochondrial function via PPAR-alpha and PGC-1. Nat Med 2011;17:1076-1085
14. Schreiber R, Diwoky C, Schoiswohl G, Feiler U, Wongsiriroj N, Abdellatif M, Kolb D, Hoeks J, Kershaw EE, Sedej S, Schrauwen P, Haemmerle G, Zechner R: Cold-Induced Thermogenesis Depends on ATGL-Mediated Lipolysis in Cardiac Muscle, but Not Brown Adipose Tissue. Cell Metab 2017;26:753-763 e757
15. Hammarstedt A, Syed I, Vijayakumar A, Eliasson B, Gogg S, Kahn BB, Smith U: Adipose tissue dysfunction is associated with low levels of the novel Palmitic Acid Hydroxystearic Acids. Sci Rep 2018;8:15757
16. Cajka T, Smilowitz JT, Fiehn O: Validating Quantitative Untargeted Lipidomics Across Nine Liquid Chromatography-High-Resolution Mass Spectrometry Platforms. Anal Chem 2017;89:12360-12368
17. Rodbell M: Metabolism of Isolated Fat Cells. I. Effects of Hormones on Glucose Metabolism and Lipolysis. J Biol Chem 1964;239:375-380
18. Kuda O, Rombaldova M, Janovska P, Flachs P, Kopecky J: Cell type-specific modulation of lipid mediator's formation in murine adipose tissue by omega-3 fatty acids. Biochem Biophys Res Commun 2016;469:731-736
19. Schweiger M, Romauch M, Schreiber R, Grabner GF, Hutter S, Kotzbeck P, Benedikt P, Eichmann TO, Yamada S, Knittelfelder O, Diwoky C, Doler C, Mayer N, De Cecco W, Breinbauer R, Zimmermann R, Zechner R: Pharmacological inhibition of adipose triglyceride lipase corrects high-fat diet-induced insulin resistance and hepatosteatosis in mice. Nat Commun 2017;8:14859
20. Zhou P, Santoro A, Peroni OD, Nelson AT, Saghatelian A, Siegel D, Kahn BB: PAHSAs enhance hepatic and systemic insulin sensitivity through direct and indirect mechanisms. J Clin Invest 2019;129:4138-4150